Oncogene (2016) **35,** 2003–2010

www.nature.com/onc

SHORT COMMUNICATION

Opposing effects of pericentrin and microcephalin on the pericentriolar material regulate CHK1 activation in the DNA damage response

AK Antonczak[1,4], LI Mullee[1,4], Y Wang[1], D Comartin[2], T Inoue[3], L Pelletier[2] and CG Morrison[1]

Genotoxic stresses lead to centrosome amplification, a frequently-observed feature in cancer that may contribute to genome instability and to tumour cell invasion. Here we have explored how the centrosome controls DNA damage responses. For most of the cell cycle, centrosomes consist of two centrioles embedded in the proteinaceous pericentriolar material (PCM). Recent data indicate that the PCM is not an amorphous assembly of proteins, but actually a highly organised scaffold around the centrioles. The large coiled-coil protein, pericentrin, participates in PCM assembly and has been implicated in the control of DNA damage responses (DDRs) through its interactions with checkpoint kinase 1 (CHK1) and microcephalin (MCPH1). CHK1 is required for DNA damage-induced centrosome amplification, whereas MCPH1 deficiency greatly increases the amplification seen after DNA damage. We found that the PCM showed a marked expansion in volume and a noticeable change in higher-order organisation after ionising radiation treatment. PCM expansion was dependent on CHK1 kinase activity and was potentiated by MCPH1 deficiency. Furthermore, pericentrin deficiency or mutation of a separase cleavage site blocked DNA damage-induced PCM expansion. The extent of nuclear CHK1 activation after DNA damage reflected the level of PCM expansion, with a reduction in pericentrin-deficient or separase cleavage site mutant-expressing cells, and an increase in MCPH1-deficient cells that was suppressed by the loss of pericentrin. Deletion of the nuclear export signal of CHK1 led to its hyperphosphorylation after irradiation and reduced centrosome amplification. Deletion of the nuclear localisation signal led to low CHK1 activation and low centrosome amplification. From these data, we propose a feedback loop from the PCM to the nuclear DDR in which CHK1 regulates pericentrin-dependent PCM expansion to control its own activation.

Oncogene (2016) **35,** 2003–2010; doi:10.1038/onc.2015.257; published online 13 July 2015

INTRODUCTION

Centrosomes are small organelles that direct microtubules in the formation of the mitotic spindle and in the organisation of the interphase cytoskeleton. Depending on cell cycle stage, they consist of two or four centrioles, which are made up of microtubule cylinders with ninefold symmetry. The centrioles are arranged within and organise the pericentriolar material (PCM), which is a highly dynamic proteinaceous assembly in which the microtubule-nucleating assemblies reside.[1] This assembly increases in size and its capacity for microtubule nucleation as mitosis initiates, a process termed centrosome maturation.[2] The PCM was frequently described as an amorphous structure because of its indistinct morphology under the electron microscope. However, recent work using subdiffraction imaging revealed high-order organisational properties of the PCM,[3–6] consistent with some earlier work indicating an underlying structure to the PCM.[7]

The microtubule anchoring and nucleation centres that are found in the PCM mean that changes in the number of centrosomes can have marked consequences on the cell.[8] Centrosome numbers are frequently altered in tumour cells, with aneuploidy and chromosomal instability being closely correlated with excess centrosomes.[9–13] Although mitotic problems leading to chromosome segregation defects are a major outcome of centrosome abnormalities,[14] cytoskeletal changes caused by centrosome amplification can also affect cell adhesion and migratory/invasive behaviour,[15,16] providing another avenue by which centrosome aberrations can contribute to tumourigenesis. For these reasons, centrosome duplication is normally tightly controlled by the cell cycle machinery.

Despite this tight control, centrosome amplification can arise from a number of sources. One such is through the DNA damage response (DDR), a complex signalling mechanism that delays cell cycle progression and initiates DNA repair pathways after genotoxic stress. CHK1 (checkpoint kinase 1), a serine–threonine kinase, is a major effector of the DDR.[17] A requirement for CHK1 has been demonstrated in centrosome amplification after a range of different genotoxic insults.[18–20] How CHK1 activation in the DDR leads to centrosome amplification is not clear. Current models include the activation of the centrosome-regulatory Cdk2 kinase[21] and the excessive assembly of centriolar satellites,[22] a process that also occurs during extended S-phase delays that permit centrosome overduplication.[23]

[1]Centre for Chromosome Biology, School of Natural Sciences, National University of Ireland Galway, Galway, Ireland; [2]Lunenfeld-Tanenbaum Research Institute, University of Toronto, Toronto, Canada and [3]Department of Cell Biology, Johns Hopkins University, Baltimore, MD, USA. Correspondence: Professor C Morrison, Centre for Chromosome Biology, National University of Ireland Galway, Biosciences Building, Dangan, Galway, Ireland.
E-mail: Ciaran.Morrison@nuigalway.ie
[4]Joint first authorship.
Received 20 October 2014; revised 3 May 2015; accepted 26 May 2015; published online 13 July 2015

Two CHK1 interactors and regulators, the PCM component, pericentrin and the tumour suppressor, MCPH1/microcephalin/Brit1 (hereafter MCPH1), also localise to the centrosome and contribute to the regulation of centrosome number.[24–27] Overexpression of pericentrin can distort the PCM and cause centrosome overduplication in S-phase-arrested cells.[3,28] However, the impact of DNA damage on the PCM is not known. Here, we set out to explore how the PCM responds to DNA damage and how pericentrin and MCPH1 affect such responses and contribute to the regulation of CHK1.

RESULTS AND DISCUSSION

To examine the impact of DNA damage on the PCM, we knocked the coding sequence for superfolding green fluorescent protein into the chicken *PCNT* locus.[27] Tagged pericentrin colocalized with centrosomal markers, indicating that it functioned normally at centrosomes (Supplementary Figure 1a). Three-dimensional structured-illumination microscopy (3D-SIM) showed that pericentrin-superfolding green fluorescent protein localised to discrete toroidal structures around the centrioles throughout the cell cycle, with an increased PCM volume seen in mitosis (Figures 1a–c), as described in previous analyses of the PCM with this technology.[3–6] Consistent with the arrangement of pericentrin within the PCM reported for human pericentrin and the *Drosophila* orthologue, PLP,[3,4] the toroid defined by visualising the C-terminal GFP tag lies within the ring seen with an antibody to the N terminus of pericentrin (Figure 1d). Thus, 3D-SIM visualisation of the PCM in chicken DT40 cells reveals that pericentrin is anchored with its C terminus at the centriole and its N terminus extending outwards to the centrosomal periphery, as is seen in other metazoan centrosomes. Next, we examined the effect of irradiation (IR) on the PCM. As shown in Figure 1e, IR treatment led to a marked dispersion and loss of discrete PCM signal that was clearly distinct from the alterations that accompany PCM maturation during the onset of mitosis, showing that one impact of the DDR is the disruption and expansion of the PCM.

We then used indirect immunofluorescence with antibodies to pericentrin and CDK5RAP2, another PCM component,[29] to image the PCM (Figure 1f and Supplementary Figure 1b). To ensure that the effects on the PCM were DDR-dependent and did not include mitotic effects on the PCM,[30] we restricted our analysis to G2 cells by examining the PCM only in cells with two centrosomes and non-condensed chromosomes. To measure changes in the PCM, three-dimensional volumes of the PCM were determined using the Volocity software (PerkinElmer, Waltham, MA, USA). After IR, the mean volume of the PCM increased significantly when measured using antibodies to either pericentrin or CDK5RAP2, plateauing by 3–4 h post-treatment (Figure 1g and Supplementary Figures 1c and d). We next sought to define the dynamics and dependencies of this expansion and dispersion of the PCM. As shown in Figure 1g, the mean CDK5RAP2-defined PCM volume in wild-type cells increased by 28% after IR. Mean PCM volumes in CHK1-deficient cells were 21% lower compared with those seen in wild-type cells before IR and showed no increase in volume after exposure. The PCM volumes in untreated pericentrin-deficient

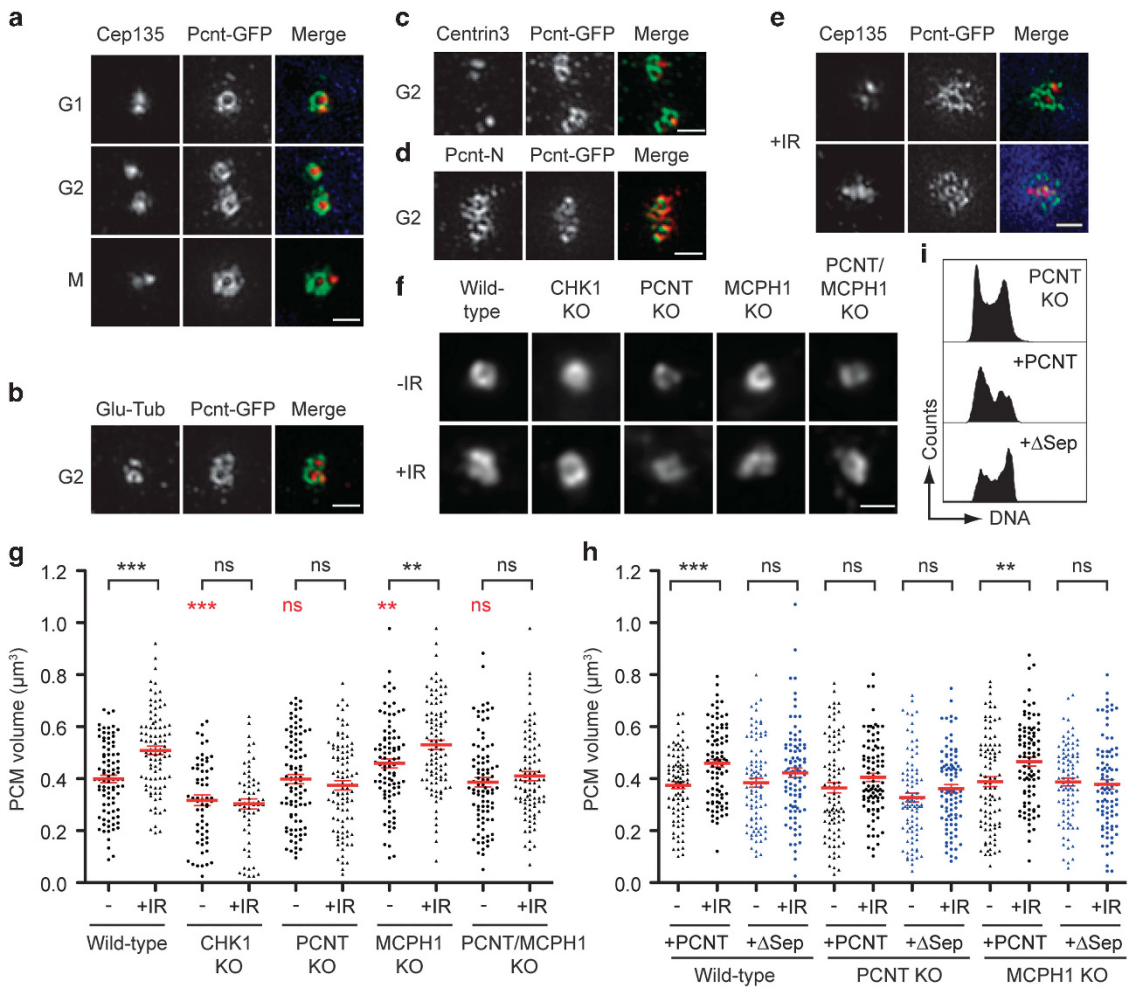

cells showed no difference from wild-type cells but exhibited no increase after IR. MCPH1 deficiency caused a significant 15% increase over wild-type cells in the mean PCM volume before IR, which was further increased by 15% after IR treatment. Interestingly, deletion of pericentrin from MCPH1-deficient cells restored the PCM volume to wild-type levels and blocked any increase in PCM volume after IR (Figure 1g). The pericentrin-defined PCM volumes showed similar trends after IR, with wild-type cells expanding by 27%, MCPH1 null by 56% and CHK1 by a nonsignificant 1% (Supplementary Figure 1c). Taken together, these results indicate that the expansion of the PCM after DNA damage requires CHK1 and pericentrin, and is restrained by MCPH1.

Recent data have indicated that separase-mediated cleavage of pericentrin leads to centriole disengagement and thus permits centriole duplication.[31–33] Separase is activated by DNA damage,[34] therefore pericentrin might be a relevant centrosomal target of the DDR. We cloned full-length pericentrin and generated a mutant without the consensus sequence for separase cleavage (ΔSep). As shown in Figure 1h, the transient expression of wild-type pericentrin had no significant impact on PCM expansion in wild-type cells or *MCPH1* knockouts. Although wild-type pericentrin expression did not significantly rescue PCM expansion in *PCNT* knockouts, which we attribute to the low level of expression attained in transient experiments, the expression of the ΔSep pericentrin mutant led to a reduced PCM expansion in wild-type and MCPH1-deficient cells (Figure 1h), suggesting that the cleavage of pericentrin is required for PCM expansion. We saw an accumulation of cells with 2C DNA content in ΔSep transfectants but not in cells that overexpressed wild-type pericentrin (Figure 1i), consistent with previous data indicating a role for pericentrin cleavage in cell cycle progression.[31,32]

The requirement for CHK1 in PCM expansion suggested that the PCM might be a target of the DDR. We therefore tested the requirement for CHK1 kinase activity and the highly conserved phosphorylation site at Ser-345 by stably expressing defined CHK1

Figure 1. PCM expansion after DNA damage requires CHK1 and pericentrin, and is restricted by MCPH1. (**a–c**) 3D-SIM microscopy of DT40 centrosomes shows toroidal PCM (anti-GFP to visualise pericentrin-GFP; green) around the centrioles ((**a**) anti-Cep135, (**b**) glutamylated tubulin, (**c**) centrin3; red) at all cell cycle stages examined. Scale bar, 0.6 μm. Superfolder GFP-expressing sequence[44] (a gift from E Tippmann) was amplified by PCR using *Taq* polymerase (Sigma-Aldrich, Dublin, Ireland) using the following primers: 5′-GGCCGCAATGGTTAGCAAAGGTGAAG-3′ and 5′-GTTAATGGTGATGATGATGGTGGCTGCC-3′ and cloned into a previously described targeting construct for the modification of the 3′ end of the *PCNT* locus.[27] For SIM imaging, DT40 cells were grown on poly-L-lysine-coated coverslips for 24 h. SIM was performed on a three-dimensional (3D) structured-illumination microscope (OMX v3; Applied Precision, Issaquah, WA, USA) as described.[3] 3D-SIM image stacks were reconstructed using the SoftWorx 5.0 software package (Applied Precision). (**d**) 3D-SIM of pericentrin in DT40 cells using antibodies to the N-terminal region (PCNT-N; green) or to the C terminus (red) confirms the exterior positioning of the N terminus of pericentrin. Scale bar, 0.6 μm. (**e**) IR-induced changes in PCM visualised by 3D-SIM of a G2 cell with antibodies to Cep135 (red) and GFP (green) 24 h after exposure to 5 Gy. Both centrosomes are shown. Scale bar, 0.6 μm. (**f**) Individual G2 centrosomes from cells of the indicated genotype, before and 4 h after 5 Gy IR, stained for CDK5RAP2. Scale bar, 1 μm. Generation of *CHK1*, *PCNT*, MCPH1 and *PCNT*/*MCPH1* mutant DT40 cell lines has been described previously, as have the *CHK1* rescue lines.[20,26,27,42] IR was performed using a ^{137}Cs source (Mainance Engineering, Hampshire, UK). Cells were adhered to poly-L-lysine slides for 15 min and then fixed for 10 min in 95% MeOH/5 mM EGTA (ethylene glycol tetraacetic acid; chilled to − 20 °C). After three phosphate-buffered saline (PBS) washes, slides were blocked in 1% bovine serum albumin (BSA)/PBS for 1 h, followed by 1 h incubation with primary antibody solution at 37 °C. After three PBS washes, the slides were incubated with secondary antibody solution for 45 min at 37 °C. The primary antibodies used for immunofluorescence analyses were: mouse anti-α-tubulin (B512; Sigma) at 1:1000; rabbit anti-CDK5Rap2 (Barr *et al*.;[29] a gift from F Gergely); mouse anti-centrin3 (M01 3E6; Abnova, Taipei, Taiwan) at 1:1000; rabbit anti-Cep135 (1420 739; Bird and Hyman;[45] a gift from Alex Bird) at 1:1000; mouse anti-γ-tubulin (GTU88; Sigma) at 1:250; goat anti-GFP (a gift from D Drechsel) at 1:1000; rabbit anti-GFP (ab6556; Abcam, Cambridge, UK) at 1:1000; rabbit anti-PCM-1 (817 (Dammermann and Merdes;[46] a gift from A Merdes) at 1:1000; rabbit anti-pericentrin (ab4448; Abcam) at 1:1000; mouse anti-pericentrin (ab28144; Abcam) at 1:200; and anti-phospho-CHK1 (Ser-345) (133D3; Cell Signaling, Danvers, MA, USA) at 1:300. Secondary antibodies labelled with FITC (fluorescein isothiocyanate) and Alexa 594 were obtained from Jackson ImmunoResearch (West Grove, PA, USA). Slides were then washed and mounted in Vectashield (Vector Laboratories, Cambridge, UK) supplemented with 1 μg/ml DAPI (4',6-diamidino-2-phenylindole). Cells were imaged using an IX81 microscope (Olympus, Tokyo, Japan) with a × 100 oil objective, NA 1.30. Volocity v6.2.1 (Improvision/Perkin-Elmer, Coventry, UK) was used to obtain and process images. (**g**) PCM volumes visualised by staining with anti-CDK5RAP2 antibodies before and 4 h after 5 Gy IR in cells of the indicated genotype. To measure PCM volumes, 15 fields containing G2 cells were captured with 0.4 μm Z-steps used to capture entire centrosomes. Images were then cropped to contain G2 centrosome pairs. Crops were then deconvolved in the red channel for PCM determination by pericentrin or CDK5RAP2 signals using Iterative Restoration in Volocity with a confidence limit of 95% and a iteration limit of 10. PCM volumes were then derived using the following three steps: remove noise from object (input: ROIs; filter: Fine filter); find objects using standard deviation intensity in red channel using lower limit of 10 and an upper limit of 100; exclude object by size $< 0.02\ \mu m^3$. Data show individual (black) and mean (red) volumes ± s.e.m. calculated from 90 G2 centrosomes in three separate experiments. Statistical comparisons indicated in red are with the untreated wild-type sample, and other comparisons are as indicated. $^{***}P < 0.001$; $^{**}P < 0.01$; NS, not significant by *t*-test. (**h**) The complete chicken *PCNT* cDNA was generated by reverse transcription-PCR (RT–PCR) on the basis of the predicted mRNA in the database. RNA was extracted from DT40 cells using TRI reagent (Ambion/Life Technologies, Dun Laoghaire, Ireland). RT was performed on 2 μg of total RNA using the Superscript Kit (Life Technologies) and PCR using KOD Hot Start (Millipore, Billerica, MA, USA). As this is a long sequence, we amplified the gene into six small fragments using the following primer pairs (1–6, F—forward; R—reverse, with lower case sequence indicating noncoding sequence added for cloning): 1 F, 5′-gtcgacgTTGTTTGTGTCTTGTACGGGATG; 1 R, 5′-CACTTAACTCTTGCCGATTTGCT-3′; 2 F, 5′-GAGCTGGAAAAACTTCAGGTCAT-3′; 2 R, 5′-CTTATGCTTCTTAATTTCTGCCTCA-3′; 3 F, 5′-ATTATGGCTGTAGAAGCAGAAGAAG-3′; 3 R, 5′-GAGAGCGTAAGTTAGAATGGTCCT-3′; 4 F, 5′-TCTAAAAGAAGAATCTGAGCGTCG-3′; 4 R, 5′-GGTCTGATGTTTGTAACTGCTCCT-3′; 5 F, 5′-GGGATTCGCCTGAGATTATGA-3′; 5 R, 5′-CTTGGGACAATAATGCTTCACAG-3′; 6 F, 5′-AGCTGTCTGTATCCTTAGAGCATGA-3′; 6 R, 5′-cctaggACAGATTTCAGAAGCATTCGGAT-3′. Sequences were cloned into pGEM-T Easy (Promega, Madison, WI, USA), sequenced and assembled by restriction ligation into pEGFP-C1, yielding pEGFP-cPCNT. The chicken *PCNT* sequence so generated has been deposited in GenBank as KM262664. A separase cleavage site mutant E_{2433}IMR-AIMA was generated by PCR with Phusion polymerase (NEB) using the following primers: 5′-ATGGCAAAACAAGATATAAGTATGGAACTTCCA-3′ and 5′-AATTGCAGGCGAATCCCATGAAGTCACATCT-3′. Transient transfections were performed by adding 2 μg of endotoxin-free DNA to 5×10^6 cells in a Nucleofector solution T (Lonza, Basel, Switzerland). Cells were then electroporated using program B-23 on a Nucleofector II (Amaxa, Lonza). PCM volumes were calculated and analysed as for (**g**). (**i**) Flow cytometry analysis of PCNT-deficient DT40 cells before and 24 h after transfection with the indicated pericentrin expression constructs. Cells were fixed in 1% formaldehyde solution for 15 min at 4 °C, and then permeabilized in 70% ethanol overnight at 4 °C before resuspension in 0.5 ml of solution containing 40 μg/ml propidium iodide (PI) and 100 μg/ml RNAse. Cell suspensions were incubated in the dark at 37 °C for 30 min before analysis on a FACSCantoA (BD, Franklin Lakes, NJ, USA). Data were analysed and presented using the FlowJo software version 7.6 (FlowJo, Ashland, OR, USA). Cells were gated on PI and GFP expression.

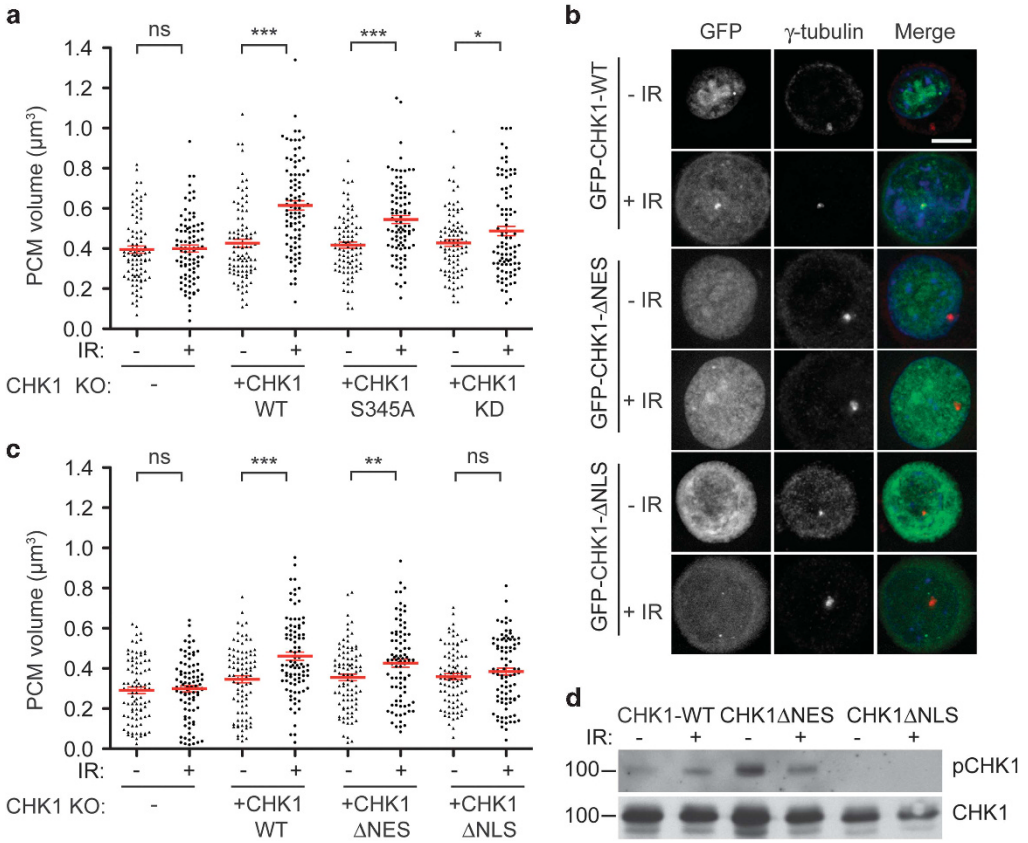

Figure 2. PCM expansion requires CHK1 but not its activity. PCM volumes visualised by staining with anti-pericentrin (**a**) or anti-CDK5RAP2 (**c**) antibodies before and 4 h after 5 Gy IR. *CHK1*-null cells were stably[20] (**a**) or transiently (**c**) transfected with *CHK1* rescue constructs. Data show individual (black) and mean (red) volumes±s.e.m. calculated from 90 G2 centrosomes in three separate experiments. ***$P < 0.001$; **$P < 0.01$; *$P < 0.05$; NS, not significant by *t*-test. (**b**) Micrographs show CHK1-deficient cells 24 h after transfection with expression plasmids for the indicated CHK1 mutant. Where indicated, cells were treated with 5 Gy. GFP-CHK1 signals are shown in green and indirect immunofluorescence detection of γ-tubulin in red. DNA was labelled with DAPI (4',6-diamidino-2-phenylindole) (blue). Scale bar, 6 μm. To generate an NES-deficient form of CHK1, we mutated the highly conserved Leu-373 and the adjacent Val-374 to Ala-Ala. The NLS mutant was generated by removing the conserved CM2 region Phe-441 to Phe-456, which contains key residues for nuclear localisation.[41] The CHK1 NES and NLS mutants were created by site-directed mutagenesis with Phusion polymerase (NEB) on pEGFP-CHK1.[47] pEGFP-CHK1-ΔNES was created using the primers 5′-CAGCGCGCCGCGAGGCGGATGA-3′ and 5′-CCACGGGCTCTGGGAGGAGCCTGG-3′ and pEGFP-CHK1-ΔNLS with 5′-CTGAAAATCAAAGGCAAACTGAGCGACGTG-3′ and 5′-GTCCACCAGGATCCTGCTCTCCAT-3′. (**d**) Immunoblot of immunoprecipitates from cells transfected with the indicated GFP-CHK1 expression constructs treated with 5 Gy and harvested 2 h later. Cells were lysed in 200 μl co-immunoprecipitation (CoIP) buffer (10 mM Tris-HCl, pH 7.5, 0.5% NP-40, 150 mM NaCl, 5 mM EDTA and protease inhibitor cocktail) for 30 min. Immunoprecipitation was then performed using GFP-Trap M beads (Chromotek, Planegg-Martinsried, Germany) (150 μg of lysate/25 μl beads) for 1 h at 4 °C. After washing, beads were boiled in 30 μl sample buffer (150 mM Tris (pH 6.8), 9% sodium dodecyl sulfate (SDS), 45% sucrose, 6 mM EDTA (pH 7.4), 0.03% bromophenol blue) for 10 min and subjected to SDS–polyacrylamide gel electrophoresis (SDS–PAGE).

mutants on a CHK1-deficient background.[20] Ser-345 mutation normally ablates CHK1 functions,[20,35] but, interestingly, it has been reported that CHK1 deficiency can be complemented by targeting a non-phosphorylatable Ser-317Ala/ Ser-345Ala mutant form to the centrosome by a PACT domain fusion.[36] As shown in Figure 2a, expression of wild-type CHK1 fully restored the PCM response to IR. Unexpectedly, both the kinase-dead and the Ser-345-Ala mutants of CHK1 supported a DNA damage-induced expansion in PCM volume, even though this response was greatly reduced in cells that expressed the kinase-dead version of CHK1. These results demonstrate that CHK1, but not necessarily its activity, is required for PCM expansion.

Where in the cell CHK1 acts to allow centrosome amplification is controversial. Both centrosomal and nuclear locations for the key Cdk1-regulatory activities of CHK1 have been indicated, with conflicting results regarding its precise localisation.[37–40] As shown in Figure 2b, GFP-tagged CHK1 localised to both the nucleus and the cytoplasm before IR. After DNA damage, however, a significant fraction localised to the centrosome, as was seen after bleomycin treatment.[36] To examine whether PCM expansion might require CHK1 outside the nucleus, we used site-directed mutagenesis to ablate the reported nuclear export signal (NES) and nuclear localisation signal (NLS) of CHK1[41] and then expressed these mutant forms of CHK1 in *CHK1*-null DT40 cells.[42] Consistent with the impact of similar mutations within the human CHK1 sequence,[41] the ΔNES form of chicken CHK1 was retained within the nucleus and the ΔNLS mutant excluded (Figure 2b). Notably, neither the NLS nor the NES mutant was observed at the centrosome, regardless of radiation treatment. However, the volume of the PCM increased after IR in cells expressing either the NLS or the NES mutant, albeit to a nonsignificant level in cells that expressed the NLS mutant (Figures 2b and c). When we examined the extent to which CHK1 became activated in response to DNA damage, we found that the radiation-induced increase in CHK1 Ser-345 phosphorylation seen in the wild-type form was abrogated by the deletion of the NLS sequence (Figure 2d). The NES deletion mutant showed a higher level of basal activation, but was not further stimulated upon IR. Taken together, these data

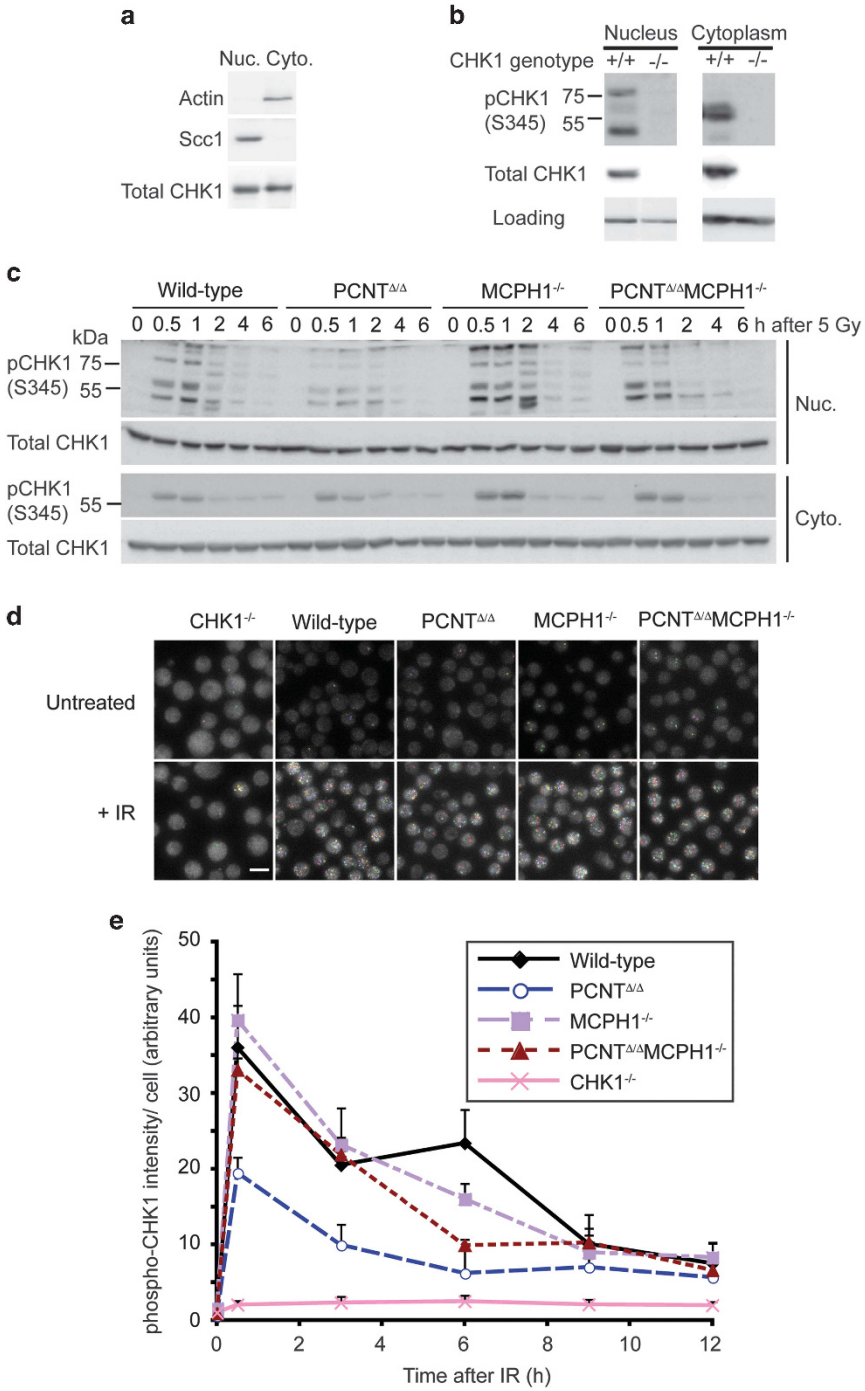

Figure 3. Opposing effects of pericentrin and MCPH1 on CHK1 activity. (**a**) Immunoblot analysis of subcellular fractionation into nuclear (Nuc.) and cytoplasmic (Cyto.) fractions. Cell fractionation experiments were performed as described previously.[48] For analysis of pEGFP-CHK1 expression, cells were transiently transfected as described above, irradiated 24 h posttransfection and harvested 2 h later. Whole-cell extracts were prepared with radioimmunoprecipitation assay (RIPA) buffer (10 mM Tris-HCl, pH 7.5, 150 mm NaCl, 5 mM EDTA, 1% sodium dodecyl sulfate (SDS), 1% Triton X-100, 1% deoxycholate and protease inhibitor cocktail), and then boiled in sample buffer for electrophoresis. Immunoblot analyses used the following primary antibodies: anti-phospho-CHK1 (Ser-345) (133D3; Cell Signaling); anti-CHK1 (DCS-310; Sigma); anti-actin (A2066; Sigma); and anti-Scc1.[49] Horse-radish peroxidase (HRP)-labelled secondary antibodies were from Jackson. (**b**) Specificity of the anti-phospho-CHK1 antibody used in immunoblots. *CHK1*$^{-/-}$ cells are shown as a negative control, with the loading controls being Scc1 for the nuclei and actin for the cytoplasmic fractions. Size markers are shown in the left (in kDa). (**c**) Time course of CHK1 activation in nuclear and cytoplasmic fractions of cells of the indicated genotype after 5 Gy IR. Size markers are shown in the left (in kDa). (**d**) Immunofluorescence microscopy of phospho-CHK1 foci in cells of the indicated genotype before and 30 min after 5 Gy IR. Nuclear IRIF identified as being above background are highlighted. Scale bar, 10 μm. (**e**) Quantitation of phospho-CHK1 IRIF in cells of the indicated genotype after 5 Gy IR. Data points are the mean ± s.d. of three experiments in which at least 4000 cells were scored per experiment. For the measurement of phospho-CHK1 focal intensities, cells were imaged by an Operetta high content imaging system (Perkin-Elmer) with a x60 air objective. Images were taken and analysed using Harmony software v3.0 (Perkin-Elmer).

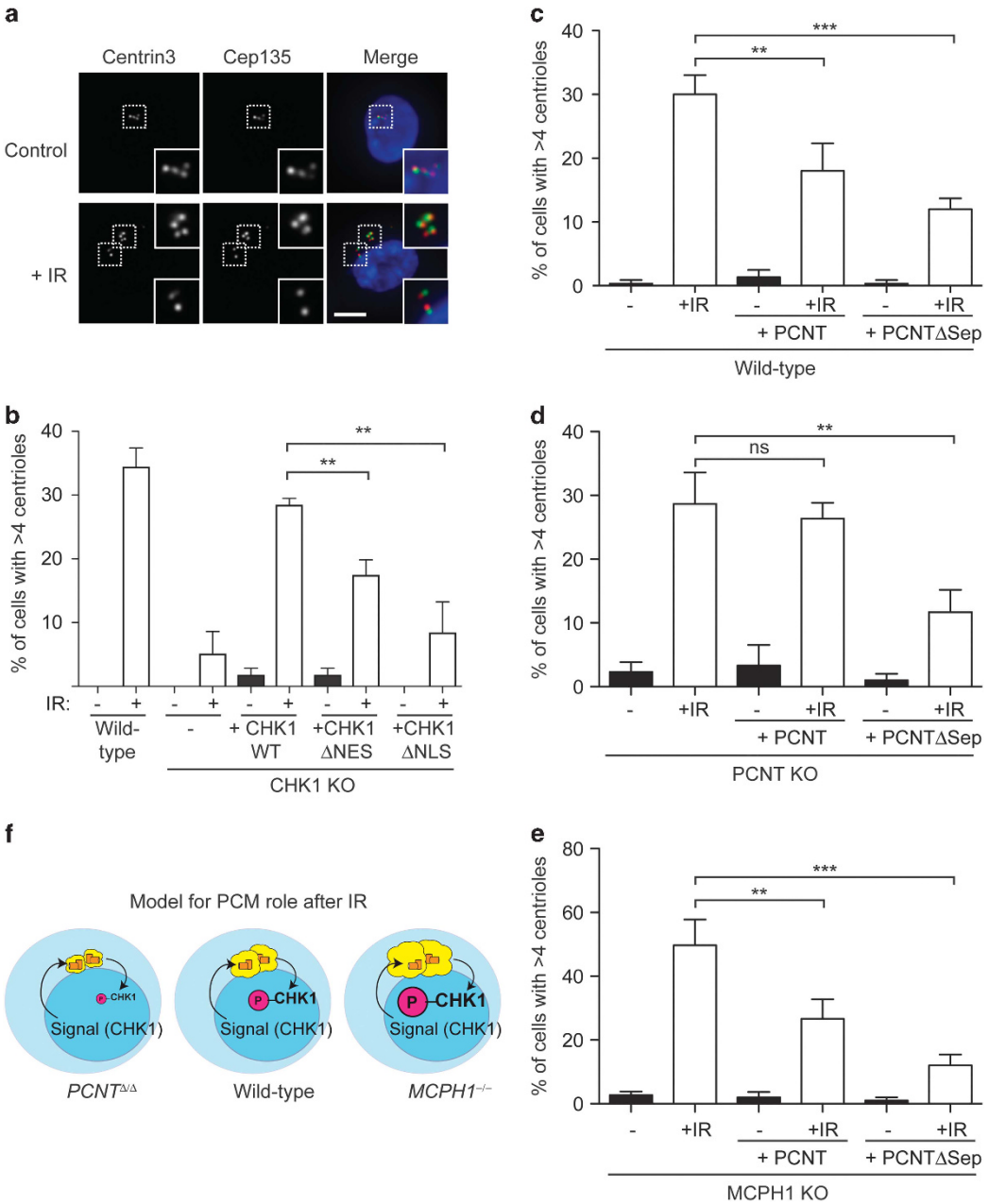

Figure 4. IR-induced centrosome amplification requires CHK1 mobility and pericentrin cleavage. (**a**) Micrograph shows centrosomes in a wild-type cell before and 24 h after 5 Gy IR treatment, stained with antibodies to centrin3 (red) and Cep135 (green), with DNA shown in blue. Scale bar, 5 μm. (**b–e**) Centrosome numbers were quantitated using antibodies to centrin3 in wild-type, and *CHK1*-, MCPH1- and *PCNT*-null cells transfected with the indicated GFP-CHK1 or GFP-pericentrin expression constructs. Histograms show mean ± s.d. of three experiments in which at least 100 cells were quantitated. ***$P < 0.001$; **$P < 0.01$; NS, not significant by *t*-test. (**f**) Model for how activated, nuclear CHK1 drives PCM expansion to permit complete activation of the nuclear DDR and how pericentrin and MCPH1 modulate this activation through the PCM.

show that PCM expansion can occur without proper CHK1 activation, but that CHK1 activation requires its appropriate, dynamic localisation between the nucleus and the cytoplasm.

Given the altered IR responses of the PCM in cells that lack pericentrin or MCPH1, we next tested how CHK1 responded to DNA damage in these mutants. In total cellular lysates, we saw no effect of pericentrin or MCPH1 deficiency on CHK1 phosphorylation after IR (data not shown). However, as this analysis would not reveal the intracellular dynamics of checkpoint activation, we performed cell fractionation experiments to separate nuclear and cytoplasmic cell components. Actin was used as a control for the cytosolic fraction and Scc1 cohesin for the nuclear components (Figure 3a). A number of different protein species were detected with the anti-phospho-CHK1 antibody that we used, particularly in the nucleus (Figure 3b). Although we do not know precisely what they represent, we consider these to be specific, because they were absent from equivalent fractions from *CHK1*$^{-/-}$ cells. A time-course analysis after 5 Gy IR revealed a weaker induction of nuclear CHK1 phosphorylation in pericentrin-deficient cells compared with that in wild-type cells, with *MCPH1*$^{-/-}$ cells showing notably more robust CHK1 activation compared with wild-type cells (Figure 3c). A less pronounced difference was seen in cytoplasmic CHK1 phosphorylation. Interestingly, the double *PCNT*$^{\Delta/\Delta}$*MCPH1*$^{-/-}$ mutants showed approximately wild-type levels of nuclear CHK1 phosphorylation, indicating that the two genes can act as suppressors of one another with respect to CHK1

activation (Figure 3c), which correlates with their effects in DNA damage-induced centrosome amplification.[27]

We next tested the localisation of phosphorylated CHK1 after IR treatment. As shown in Figure 3d, antibodies to Ser-345-phosphorylated CHK1 detected robust induction of nuclear foci in irradiated cells. We did not see any signal at centrosomes under these conditions. These foci colocalised with γ-H2AX (data not shown) and, while some background signal was detected in *CHK1*$^{-/-}$ DT40 cells, this did not increase after IR (Figures 3d and e). Although these data contrast with a previous analysis in bromodeoxyuridine-sensitised, microirradiated U2OS cells, which found that CHK1 did not localise to breaks,[43] we conclude that IR-induced foci (IRIF) of phosphorylated CHK1 at the sites of DNA damage are still being detected. Quantitating the cellular intensity of the phospho-CHK1 IRIF, we found that pericentrin deficiency greatly attenuated the activation of CHK1 over time after 5 Gy IR. This activation was restored by the deletion of *MCPH1* (Figures 3d and e). Taken together with the centrosome amplification data and our previous analysis that demonstrated a sustained CHK1 activation in the absence of *MCPH1*,[26] these observations suggest that pericentrin is necessary for full CHK1 activity and that MCPH1 normally restricts CHK1 activation. With the impact that pericentrin deficiency has on the PCM, it is possible that CHK1 activation occurs, at least in part, at the centrosome in a pericentrin-dependent manner.

We next analysed the levels of DNA damage-induced centrosome amplification as an additional readout of CHK1 activity. We have previously shown that CHK1 kinase, its activity and the phosphorylation site at Ser-345 are required to allow centrosome amplification after DNA damage.[20,21] We observed no significant centrosome amplification in cells that expressed the CHK1 NLS mutant, in keeping with the lack of CHK1 activation (Figures 4a and b). Interestingly, expression of the NES mutant significantly reduced cells' capacity for centrosome amplification after IR, suggesting that the extranuclear movement of CHK1 is required to allow control levels of centrosome amplification in response to IR treatment. These data indicate a separation of CHK1-dependent functions at the centrosome: PCM expansion, which requires CHK1 but not its activity, is not sufficient to allow centrosome amplification in the absence of CHK1 activation.

Similar to PCM expansion (Figure 1g), centrosome amplification was potentiated by MCPH1 deficiency and suppressed by loss of pericentrin.[27] Pericentrin overexpression reduced DNA damage-induced centrosome amplification in wild-type and MCPH1-deficient cells, but had no impact on amplification in a pericentrin-deficient cell background (Figures 4c–e). However, overexpression of the mutant that lacked the separase cleavage site caused a significant reduction in centrosome amplification on all three backgrounds (Figures 4c–e). These data implicate the PCM in controlling centrosomal amplification after DNA damage. Although centrosome amplification occurred normally in pericentrin-deficient cells,[27] we suggest that the cleavage of existing pericentrin, and thus the dynamic alteration of the PCM, may potentiate amplification in a manner not seen where cells have none to begin with. With the data available, our model thus suggests that PCM expansion, through separase-regulated pericentrin cleavage, stabilises an activated, centrosomal CHK1 signal that is normally downregulated through MCPH1 (Figure 4f). Our results support the existence of a feedback loop between PCM expansion and centrosomal CHK1 activity that ensures a checkpoint signal within the nucleus.

CONFLICT OF INTEREST

The authors declare no conflict of interest.

ACKNOWLEDGEMENTS

We are grateful to Alex Bird, David Drechsel, Fanni Gergely, Andreas Merdes and Eric Tippmann for reagents and to Brian McStay and Noel Lowndes for critically reading the manuscript. AKA received an EMBO Long-term Postdoctoral Fellowship and a Travelling Fellowship from the Journal of Cell Science. LIM received a Travelling Studentship from the National University of Ireland. This work was supported by Science Foundation Ireland Principal Investigator awards 08/IN.1/B1029 and 10/IN.1/B2972.

REFERENCES

1 Nigg EA, Raff JW. Centrioles, centrosomes, and cilia in health and disease. *Cell* 2009; **139**: 663–678.
2 Palazzo RE, Vogel JM, Schnackenberg BJ, Hull DR, Wu X. Centrosome maturation. *Curr Top Dev Biol* 2000; **49**: 449–470.
3 Lawo S, Hasegan M, Gupta GD, Pelletier L. Subdiffraction imaging of centrosomes reveals higher-order organizational features of pericentriolar material. *Nat Cell Biol* 2012; **14**: 1148–1158.
4 Mennella V, Keszthelyi B, McDonald KL, Chhun B, Kan F, Rogers GC *et al.* Subdiffraction-resolution fluorescence microscopy reveals a domain of the centrosome critical for pericentriolar material organization. *Nat Cell Biol* 2012; **14**: 1159–1168.
5 Fu J, Glover DM. Structured illumination of the interface between centriole and peri-centriolar material. *Open Biol* 2012; **2**: 120104.
6 Sonnen KF, Schermelleh L, Leonhardt H, Nigg EA. 3D-structured illumination microscopy provides novel insight into architecture of human centrosomes. *Biol Open* 2012; **1**: 965–976.
7 Dictenberg JB, Zimmerman W, Sparks CA, Young A, Vidair C, Zheng Y *et al.* Pericentrin and gamma-tubulin form a protein complex and are organized into a novel lattice at the centrosome. *J Cell Biol* 1998; **141**: 163–174.
8 Anderhub SJ, Kramer A, Maier B. Centrosome amplification in tumorigenesis. *Cancer Lett* 2012; **322**: 8–17.
9 D'Assoro AB, Lingle WL, Salisbury JL. Centrosome amplification and the development of cancer. *Oncogene* 2002; **21**: 6146–6153.
10 Lingle WL, Lutz WH, Ingle JN, Maihle NJ, Salisbury JL. Centrosome hypertrophy in human breast tumors: implications for genomic stability and cell polarity. *Proc Natl Acad Sci USA* 1998; **95**: 2950–2955.
11 Pihan GA, Purohit A, Wallace J, Malhotra R, Liotta L, Doxsey SJ. Centrosome defects can account for cellular and genetic changes that characterize prostate cancer progression. *Cancer Res* 2001; **61**: 2212–2219.
12 Duensing S, Lee LY, Duensing A, Basile J, Piboonniyom S, Gonzalez S *et al.* The human papillomavirus type 16 E6 and E7 oncoproteins cooperate to induce mitotic defects and genomic instability by uncoupling centrosome duplication from the cell division cycle. *Proc Natl Acad Sci USA* 2000; **97**: 10002–10007.
13 Nigg EA. Centrosome aberrations: cause or consequence of cancer progression? *Nat Rev Cancer* 2002; **2**: 815–825.
14 Ganem NJ, Godinho SA, Pellman D. A mechanism linking extra centrosomes to chromosomal instability. *Nature* 2009; **460**: 278–282.
15 Kushner EJ, Ferro LS, Liu JY, Durrant JR, Rogers SL, Dudley AC *et al.* Excess centrosomes disrupt endothelial cell migration via centrosome scattering. *J Cell Biol* 2014; **206**: 257–272.
16 Godinho SA, Picone R, Burute M, Dagher R, Su Y, Leung CT *et al.* Oncogene-like induction of cellular invasion from centrosome amplification. *Nature* 2014; **510**: 167–171.
17 Bartek J, Lukas J. Chk1 and Chk2 kinases in checkpoint control and cancer. *Cancer Cell* 2003; **3**: 421–429.
18 Loffler H, Bochtler T, Fritz B, Tews B, Ho AD, Lukas J *et al.* DNA damage-induced accumulation of centrosomal Chk1 contributes to its checkpoint function. *Cell Cycle* 2007; **6**: 2541–2548.
19 Robinson HM, Black EJ, Brown R, Gillespie DA. DNA mismatch repair and Chk1-dependent centrosome amplification in response to DNA alkylation damage. *Cell Cycle* 2007; **6**: 982–992.
20 Bourke E, Dodson H, Merdes A, Cuffe L, Zachos G, Walker M *et al.* DNA damage induces Chk1-dependent centrosome amplification. *EMBO Rep* 2007; **8**: 603–609.
21 Bourke E, Brown JA, Takeda S, Hochegger H, Morrison CG. DNA damage induces Chk1-dependent threonine-160 phosphorylation and activation of Cdk2. *Oncogene* 2010; **29**: 616–624.
22 Loffler H, Fechter A, Liu FY, Poppelreuther S, Kramer A. DNA damage-induced centrosome amplification occurs via excessive formation of centriolar satellites. *Oncogene* 2013; **32**: 2963–2972.
23 Prosser SL, Straatman KR, Fry AM. Molecular dissection of the centrosome overduplication pathway in S-phase-arrested cells. *Mol Cell Biol* 2009; **29**: 1760–1773.

24 Alderton GK, Galbiati L, Griffith E, Surinya KH, Neitzel H, Jackson AP *et al*. Regulation of mitotic entry by microcephalin and its overlap with ATR signalling. *Nat Cell Biol* 2006; **8**: 725–733.
25 Griffith E, Walker S, Martin CA, Vagnarelli P, Stiff T, Vernay B *et al*. Mutations in pericentrin cause Seckel syndrome with defective ATR-dependent DNA damage signaling. *Nat Genet* 2008; **40**: 232–236.
26 Brown JA, Bourke E, Liptrot C, Dockery P, Morrison CG. MCPH1/BRIT1 limits ionizing radiation-induced centrosome amplification. *Oncogene* 2010; **29**: 5537–5544.
27 Wang Y, Dantas TJ, Lalor P, Dockery P, Morrison CG. Promoter hijack reveals pericentrin functions in mitosis and the DNA damage response. *Cell Cycle* 2013; **12**: 635–646.
28 Loncarek J, Hergert P, Magidson V, Khodjakov A. Control of daughter centriole formation by the pericentriolar material. *Nat Cell Biol* 2008; **10**: 322–328.
29 Barr AR, Kilmartin JV, Gergely F. CDK5RAP2 functions in centrosome to spindle pole attachment and DNA damage response. *J Cell Biol* 2010; **189**: 23–39.
30 Lee K, Rhee K. PLK1 phosphorylation of pericentrin initiates centrosome maturation at the onset of mitosis. *J Cell Biol* 2011; **195**: 1093–1101.
31 Lee K, Rhee K. Separase-dependent cleavage of pericentrin B is necessary and sufficient for centriole disengagement during mitosis. *Cell Cycle* 2012; **11**: 2476–2485.
32 Matsuo K, Ohsumi K, Iwabuchi M, Kawamata T, Ono Y, Takahashi M. Kendrin is a novel substrate for separase involved in the licensing of centriole duplication. *Curr Biol* 2012; **22**: 915–921.
33 Agircan FG, Schiebel E. Sensors at centrosomes reveal determinants of local separase activity. *PLoS Genet* 2014; **10**: e1004672.
34 Prosser SL, Samant MD, Baxter JE, Morrison CG, Fry AM. Oscillation of APC/C activity during cell cycle arrest promotes centrosome amplification. *J Cell Sci* 2012; **125**: 5353–5368.
35 Wilsker D, Petermann E, Helleday T, Bunz F. Essential function of Chk1 can be uncoupled from DNA damage checkpoint and replication control. *Proc Natl Acad Sci USA* 2008; **105**: 20752–20757.
36 Niida H, Katsuno Y, Banerjee B, Hande MP, Nakanishi M. Specific role of Chk1 phosphorylations in cell survival and checkpoint activation. *Mol Cell Biol* 2007; **27**: 2572–2581.
37 Kramer A, Mailand N, Lukas C, Syljuasen RG, Wilkinson CJ, Nigg EA *et al*. Centrosome-associated Chk1 prevents premature activation of cyclin-B-Cdk1 kinase. *Nat Cell Biol* 2004; **6**: 884–891.
38 Tibelius A, Marhold J, Zentgraf H, Heilig CE, Neitzel H, Ducommun B *et al*. Microcephalin and pericentrin regulate mitotic entry via centrosome-associated Chk1. *J Cell Biol* 2009; **185**: 1149–1157.
39 Matsuyama M, Goto H, Kasahara K, Kawakami Y, Nakanishi M, Kiyono T *et al*. Nuclear Chk1 prevents premature mitotic entry. *J Cell Sci* 2011; **124**: 2113–2119.
40 Gruber R, Zhou Z, Sukchev M, Joerss T, Frappart PO, Wang ZQ. MCPH1 regulates the neuroprogenitor division mode by coupling the centrosomal cycle with mitotic entry through the Chk1-Cdc25 pathway. *Nat Cell Biol* 2011; **13**: 1325–1334.
41 Wang J, Han X, Feng X, Wang Z, Zhang Y. Coupling cellular localization and function of checkpoint kinase 1 (Chk1) in checkpoints and cell viability. *J Biol Chem* 2012; **287**: 25501–25509.
42 Zachos G, Rainey MD, Gillespie DA. Chk1-deficient tumour cells are viable but exhibit multiple checkpoint and survival defects. *EMBO J* 2003; **22**: 713–723.
43 Bekker-Jensen S, Lukas C, Kitagawa R, Melander F, Kastan MB, Bartek J *et al*. Spatial organization of the mammalian genome surveillance machinery in response to DNA strand breaks. *J Cell Biol* 2006; **173**: 195–206.
44 Pedelacq JD, Cabantous S, Tran T, Terwilliger TC, Waldo GS. Engineering and characterization of a superfolder green fluorescent protein. *Nat Biotechnol* 2006; **24**: 79–88.
45 Bird AW, Hyman AA. Building a spindle of the correct length in human cells requires the interaction between TPX2 and Aurora A. *J Cell Biol* 2008; **182**: 289–300.
46 Dammermann A, Merdes A. Assembly of centrosomal proteins and microtubule organization depends on PCM-1. *J Cell Biol* 2002; **159**: 255–266.
47 Zachos G, Black EJ, Walker M, Scott MT, Vagnarelli P, Earnshaw WC *et al*. Chk1 is required for spindle checkpoint function. *Dev Cell* 2007; **12**: 247–260.
48 Wang Y-D, Caldwell RB. Isolation of nuclear and cyotplasmic proteins from DT40 cell lines. In: Buerstedde J-M, Takeda S (eds). *Reviews and Protocols in DT40 Research*. Springer: New York, NY, USA, 2006, pp 439–441.
49 Stephan AK, Kliszczak M, Dodson H, Cooley C, Morrison CG. Roles of vertebrate smc5 in sister chromatid cohesion and homologous recombinational repair. *Mol Cell Biol* 2011; **31**: 1369–1381.

Supplementary Information accompanies this paper on the Oncogene website (http://www.nature.com/onc)